1   Process characteristics for microwave assisted hydrothermal carbonization of cellulose

2   Junting Zhang[a,c], Ying An[b], Aiduan Borrion[c], Wenzhi He[a], Nan Wang[a], Yirong Chen[d], Guangming Li[a]*

3   [a]* College of Environmental Science and Engineering, Tongji University, 1239 Siping Road, Shanghai, 200092, China
4   [b] Shanghai Shendi Institute, Shanghai, 200120, China
5   [c] Department of Civil, Environmental and Geomatic Engineering, University College London, Gower Street, London,
6   WC1E 6BT, UK
7   [d] College of Natural Resources, University of California, Berkeley, 260 Mulford Hall, CA, 94704, USA

8

9   **1. Introduction**

10   Hydrothermal carbonization (HTC) as a promising technology for biomass

11   enhancement (Kambo and Dutta, 2014; Kim et al., 2016; Lynam et al., 2014), and

12   organic waste treatment (Berge et al., 2011; Goto et al., 2004; Lu et al., 2012) has

13   gained significant attention in recent years. HTC is a novel thermal conversion process

14   under relatively low temperature(180-$350^{\circ}C$) for conversion of waste streams to value-

15   added products (Berge et al., 2015). During this process, energy is maintained within

16   solid product known as 'hydrochar'(Lu et al., 2012) to obtain better energy properties

17   and maximize the added value of recovery products (Fava et al., 2015). Cellulose as the

18   most copious natural raw material and one of the basic constituents of lignocellulosic

19   materials(Suhas et al., 2016), has been studied widely as an ideal feedstock for process

20   analysis(Lu et al., 2013) and kinetics study(Álvarez-Murillo et al., 2016) of HTC

21   treatment.

22   The early mechanism of HTC proposed by Sevilla and Fuertes (2009) indicated that the

23   formation of hydrochar from HTC of cellulose generally followed a series of reactions,

including hydrolysis, dehydration and fragmentation into soluble products,

polymerization or condensation of soluble products and finally resulted in growth of

solid spheres by aromatization and nucleation. However, Falco et al. (2011) argued

that this cellulose dissolution mechanism could hardly explain the observed well-

developed aromatic nature of hydrochar at early stage of HTC reaction. Instead, their

study revealed a pyrolysis-like mechanism with intramolecular condensation,

dehydration and decarbonisation reactions, with a primary contribution in hydrochar

formation between 200℃ and 280℃. García-Bordejé et al. (2017) proposed that these

two mechanisms co-exist as 'soluble pathway' in solution after cellulose hydrolysis and

'solid pathway' in solid phase . Since the predominant mechanism depends on

variations in the individual rates of these two co-existent pathways(García-Bordejé et

al., 2017), the kinetics description of this reaction network is essential to provide

insights into the mechanism of HTC. Previously the kinetics of HTC process were

generally studied by mass-loss in solid phase (Álvarez-Murillo et al., 2016; Reza et al.,

2013). The simulation approach using weight lost for calculation is intuitive, however,

ignores the effect of cellulose hydrolysis and importance of carbon content, which is a

representative feature of hydrochar presented in quantities of researches(Jatzwauck

and Schumpe, 2015). Thus the concentration of carbon was introduced into kinetics

calculation by Jatzwauck and Schumpe (2015). This calculation method uses the

information from both carbon content and weight loss to describe the progress of HTC

reaction, which is also adapted in the present research.

Unlike conventional time-consuming HTC process, microwave assisted hydrothermal

carbonization (MAHTC) is considered as a potentially faster, more efficient and

2

selective method (Fan et al., 2013). Studies have shown that MAHTC could succeed in recovering valuable products from pure carbohydrates, e.g. glucose and cellulose (Fan et al., 2013) and a variety of organic waste such as lignocellulosic waste (Elaigwu and Greenway, 2016; Klein et al., 2016), waste paper (Hassanzadeh et al., 2015), fish waste(Kannan et al., 2017) as well as human bio-waste (Afolabi et al., 2017; Ood and Sohail, 2017). The potential of the microwave-assisted reaction to effectively decrystallize, dissolute, and depolymerize cellulose at relatively low temperatures and under mild reaction conditions has been reported in recent researches(Fan et al., 2013; Hassanzadeh et al., 2015). Compared with conventional heating mode, microwave greatly enhanced reducing sugars yields of process water (Richel et al., 2011), and significantly shortened reaction time for HTC (Elaigwu and Greenway, 2016), resulting in enhancement of reaction rates. Since most studies were focused on the characteristics of products rather than understanding of process kinetics, the effects of reaction conditions of MAHTC on the yield and quality of hydrochar has not been evaluated properly.

For both HTC and MAHTC, understanding of hydrochar characteristics and reaction kinetics are necessary for reactor design and optimization. Although the two parallel pathways - the 'soluble pathway' and 'solid pathway' have been proposed for HTC of cellulose, no kinetics studies of these two pathways have been published. Furthermore, there is a lack of understanding on the effect of microwave on the HTC process. Therefore, the aim of this work is to provide fully understanding of MAHTC with process analysis and kinetics study. The novelty of this study is reflected in the following three objectives: (1) to examine the process characteristics with chemical

70 composition and general properties of hydrochar generated from MAHTC of cellulose,

71 (2) to provide a first order kinetics for MAHTC of cellulose based on carbon

72 concentration giving insights into the mechanism of both 'soluble pathway' and 'solid

73 pathway', (3) to study the impact of microwave heating on HTC process with

74 comparative kinetics analyses from the present and previous models.

75 **2. Materials and methods**

76 2.1 Microwave-assisted hydrothermal carbonization reactor

77 A schematic diagram of the MAHTC reactor is shown in Figure 1, including a stainless-

78 steel autoclave, a microwave magnetron (designed microwave power of 1000W), an

79 electronic heater (designed power of 500W), two temperature indicators, a

80 mechanical stirrer (500rpm) and a control box. MAHTC of cellulose was conducted in

81 the quartz glass vessel of 500ml, which was just the size to fit in and sealed inside the

82 autoclave. The magnetron was set up at the bottom of the autoclave to generate

83 microwave heating though the vessel. The electronic heater was set up at the outer

84 wall of autoclave. Two temperature sensors were placed to detect the real-time

85 temperature of the centre and outer wall of the reactor. Unlike previous studies, the

86 internal temperature was defined as the reaction temperature in this study to consider

87 the volumetric thermal effects from microwave heating (De la Hoz et al., 2005).

88 The rate of microwave power was set at 1000W during heating process. During pre-

89 experiment, microwave heating showed great advantages on traditional electronic

90 heating method from centre temperature range of 0-100℃, however, the heating rate

91 began to decrease afterwards until the outer wall of reactor has reached similar

4

92   temperature of the centre. In order to speed up the heating process, 500W electronic

93   heating was provided through the side wall of reactor to reach the designed

94   temperature within half an hour. Thus the heating process was assumed to be

95   negligible in this study and the time when the centre of reactor reached the desired

96   temperature was defined as t=0 min on the time scale. The control box has control of

97   the temperature, microwave power and the stirrer. The maximum working

98   temperature and pressure are 300℃ and 8MPa respectively.

99   2.2 Microwave-assisted hydrothermal carbonization process

100   Microcrystalline cellulose (Sigma-Aldrich) was used as feedstock for MAHTC and dried

101   at 105℃ until constant weight for further analysis. Deionized water was loaded in the

102   reactor as reaction medium. MAHTC was performed in the reactor with 10g

103   microcrystalline cellulose and 300ml hot compressed water added in the quartz

104   chamber. Reaction temperatures from 220℃ to 250℃ and the residence time up to 2

105   hours with interval of 30 minutes were used to evaluate the effect of reaction

106   conditions in this study. After reaching desired temperature, only microwave heating

107   was used during reaction process to withstand the anticipated temperatures and

108   pressures. Different range of microwave power was used in the experiment, starting

109   from 550W to 850W, to offset the heat loss and maintain certain reaction temperature

110   from 220 to 250℃. Thus the microwave power was relatively constant with control of

111   ±50W when the total heating system reached a dynamic balance during MAHTC

112   process.

113   After reaching the desired reaction time, the microwave-heating system of reactor was

114   immediately turned off and a cooling fan started working. It was observed from the

115   display temperature on the control box that the internal temperature could drop to

116   under 180℃ within about 10 minutes, after which it was assumed that the main HTC

117   reactions had stopped (Reza et al., 2013). The quartz chamber was taken out of the

118   autoclave after the reactor was observed to reach room temperature. The solids were

119   separated by vacuum filtration using a 0.45μm hydrophobic membrane and washed

120   with 100ml of deionized water afterwards. The solid samples were dried at 105℃ for

121   24 h and stored in a dryer for further analysis. All experiments were performed in

122   triplicate to obtain an average data.

123   2.3 Characteristics of hydrochar

124   The element analysis of the feedstock and hydrochar were obtained by a Vario EL III

125   Element Analyzer (Elementar Analysensysteme GmbH, Germany) to determine the

126   weight percentage of hydrogen, nitrogen and carbon, according to ASTM D5373-08.

127   The solid yield is defined as below,

128    $Solid\ Yield = \dfrac{m_s}{m_0} \times 100\%$

129   Where m_s is the mass of solid residue and m_0 is the initial mass of cellulose, which is

130   10g of each experiment in this study.

131   High heating value (HHV) of samples was determined using a bomb calorimeter and

132   the energy retention efficiency is a measure of the fraction of feedstock energy

133   retained within the solid material(Lu et al., 2013), which is defined as the given

134   formula below.

135    $Energy\ Rentention\ Efficiency = \frac{HHV_S}{HHV_0} \times Solid\ Yield$

136   Where HHV_S and HHV_0 are the high heating value of the solid residue and cellulose

137   respectively.

138   **3. Results and discussion**

139   3.1 Microwave-assisted hydrothermal carbonization of cellulose

140   3.1.1 Solid decomposition during MAHTC

141   Effects of reaction temperature and retention time of MAHTC on solid yield generation

142   were presented in Figure 2.a. As suggested in previous research(Diakité et al., 2013), it

143   was clear that longer residence time and higher reaction temperatures led to more

144   carbonization of the feedstock and as a consequence, lower hydrochar mass yields.

145   The solid yield of hydrochar under 220℃ and 230℃ showed similar trends to gradually

146   decrease with reaction time and finally ends with more than 50% solid loss in

147   feedstock. When temperature reached 240℃ and above, the solid yield decreased

148   rapidly in the first 30 minutes with more than 50% mass loss and changed less

149   dramatically afterwards to the final solid yield of 40%. The rapid decreasing in solid

150   yield of hydrochar samples, which suggests a start time of major decomposition in

151   cellulose(Danso-Boateng et al., 2013), were observed between 90-120 min at 220℃,

152   30-60 min at 230℃ and within 30 mins at 240 and 250℃. Thus an acceleration by high

153   temperature on cellulose decomposition was indicated by the advanced start time.

154　Another effect of high temperature on solid decomposition was observed at t=0 min in

155　Figure 2.b by the decreased solid yield, that the solubilisation extent of feedstock was

156　enhanced with increased temperature during heating process. Similarly, the decreased

157　solid yield in the first hour (at t=30 min and t=60 min in Figure 2.b) further illustrated

158　the effect of high temperatures on accelerating the degradation of feedstock.

159　Experiments under 260 and 270℃ were conducted as well and the results showed a

160　faster degradation in the first 30 mins, however, the solubilisation of feedstock was so

161　severe that under both temperature the solid yields could reach below 60% at t=0 min.

162　It can be confirmed that to continue increasing the temperature could further

163　accelerate the reaction, however, the results are not comparable with these obtained

164　under lower temperatures and not applicable for further kinetics calculation in this

165　study.

166　It should be noted that under all the circumstance the solid yields of hydrochar

167　samples could reach a similar value of 40% after 2 hours (at t=120 min in Figure 2.b).

168　Therefore it is suggested that a relatively stable stage would be reached in the end as a

169　result of enough extension of reaction time, though the retention time always showed

170　less pronounced effect than temperature on solids degradation in previous

171　research(Danso-Boateng et al., 2013). In this study, the previously reported(Sevilla and

172　Fuertes, 2009) increasing of solid yield as a result of condensation and polymerization

173　of soluble fractions during 'soluble pathway' was not observed, indicating it was not

174　the dominant mechanism here. The answer of the question whether the increasing of

175　solid yield can be found with further extension of reaction time is likely to be negative.

176　Because the relatively stable stages showed that HTC reactions were almost completed

177 within the experiment scope in this study. The observed solid yields in this research

178 resemble the results of previous studies using conventional HTC method under similar

179 reaction temperature (Álvarez-Murillo et al., 2016; García-Bordejé et al., 2017), where

180 the reaction time to reach the similar reaction extent were substantially shortened

181 from 10-20 hours to 1-2 hours by MAHTC. Although the resulting solid yields would

182 vary in some extent because of the different parameters of reactors, the big

183 differences between these results still highlight the acceleration effects of microwave

184 on HTC process.

185 3.1.2 Carbon content and energy properties of hydrochar

186 Previous research (Sevilla and Fuertes, 2009) using conventional HTC method has

187 proved that increasing reaction temperature and retention time lead to high carbon

188 content in hydrochar. Similar trend was observed here that the highest carbon content

189 of 72.5% was obtained at 250℃ for 120 minutes, which is respectively the highest

190 reaction temperature and longest retention time within the scope of this study. After

191 microwave assisted HTC process for 120 minutes, the carbon content increased from

192 43.1% in the pure cellulose to 53.1% to 72.5% in the hydrochar samples. The distinct

193 increase of carbon content with reaction time in Figure 3.a illustrated the time when

194 major carbonization process took place, during which the initial feedstocks

195 transformed into carbon-enriched products. This process was observed to be highly

196 effected by reaction temperature as well. The change of carbon content was barely

197 observed under 220℃ implying hydrolysis was the main reaction path during

198 solubilisation of cellulose at 220℃. On the contrary, the carbonization process was

199 accelerated to take place in the first 30 minutes under 240 and 250℃ shown by the

200 rapid increase of carbon content in the samples. In addition, the change of carbon

201 content turned to be evident that the remaining solids were comprised of both

202 unreacted cellulose and hydrochar (Álvarez-Murillo et al., 2016). Therefore the

203 proposed kinetic model should consider not only the remaining quantity of solids but

204 also the distribution of these two components (i.e. feedstock and solid product).

205 The observed trend of carbon content was consistent with the reaction process

206 illustrated by degradation of solid yield that the rapid change in both indicators

207 occurred within similar time range under specific reaction temperature. However,

208 though the solid yield had decreased from 100% to 80% at t=0 min during heating

209 time, the results of carbon content showed relatively constant at t=0 min (see Figure

210 3.a). Thus it was assumed that only slight dissolution took place during heating process

211 and its effect on carbonization process could be ignored in this study. The extension of

212 reaction time did not show obvious effects on carbon enrichment of hydrochar after

213 30 minutes under 240 and 250℃, indicating that the carbonization reaction had

214 achieved balance. Therefore, the value of the highest measured carbon content can be

215 defined as pure hydrochar products (Jatzwauck and Schumpe, 2015) after MAHTC of

216 cellulose under experiment conditions. The resulting highest carbon content of 72.5%

217 in this study resembles to the value of these hydrochar samples generated from

218 conventional HTC after 6.8(Álvarez-Murillo et al., 2016) and 20 hours(Kang et al., 2012)

219 reaction under 245℃, providing another proof to support the accelerating effect of

220 microwave assisted heating during HTC process.

221 The high heating values (HHV) is the absolute quantity of energy that is present in a

222 sample thus a fundamental feature of the hydrochar according to Elaigwu et al.(2016).

223 The extent of the bars in Figure 3.b presents the HHV of hydrochar samples generated

224 under different reaction conditions with its corresponding energy retention efficiency.

225 In this study, we obtained the highest HHV of 26.31 MJ/kg by MAHTC under 250℃ for

226 120 min, which obtained a 50% increase compared to that of conventional HTC

227 method under similar condition (Álvarez-Murillo et al., 2016). An average value of 25

228 MJ/kg of conventional HTC generated hydrochar after 96 hours reaction under 225℃

229 to 275℃ was reported by Lu et.al (2013), which is another evidence of the

230 enhancement effect of microwave heating on hydrochar properties. As shown in

231 Figure 2.b, the HHV value went through an apparent rise with increasing temperature

232 between 30 min to 90 min, while the differences were not obvious at t=0 min and

233 t=120 min (from 230 to 250℃). The relatively unchanged HHV values at these two

234 times can respectively assign to the initial state and final state of MAHTC reaction

235 (without considering the heating process), between which is considered as an ideal

236 period for kinetic study of MAHTC.

237 In the case of energy retention efficiency, the combined action of feedstock

238 solubilisation and hydrochar generation processes resulted in the observed variation

239 under different reaction temperature. It was different from results of Lu et al.(2013)

240 that the energy retention efficiency was similar at all reaction temperatures, indicating

241 these two reactions had been accelerated by high temperatures. The sharp decreasing

242 trend in energy retention efficiency with increasing temperature within short retention

243 time suggested carbon transition from solid to liquid and gas phase, which was the

244 predominant pathway at early reaction stage. The latter stage was instead presumed

245 to be dominated by carbon-enrichment reaction resulting in increasing of energy

246 retention efficiency. As previously discussed in the introduction, the predominant

247 mechanism depends on variations in the individual rates of the two co-existent

248 pathways, which are shown to be highly effected by reaction temperature in the

249 present research. It should be noticed as well that the energy retention efficiency

250 decreased with extension of time under all the temperatures. The explanation could

251 be increasing transition into gas phase and resulted in formation of carbon dioxide

252 with longer reaction time (Hoekman et al., 2011; Lu et al., 2013). Thus the favourable

253 condition for energy-enriched product by MAHTC of cellulose should be 250℃ for 90

254 min, considering both HHV and energy retention efficiency for optimisation.

255 As already suggested, the HHV results showed that at 220℃ and at t=0 min under all

256 the temperature, the remaining solid residues were barely affected by the MAHTC

257 treatment because no solids conversion but only cellulose solubilisation has occurred

258 (Lu et al., 2013). As a matter of fact, though we observed an obvious decreasing solid

259 yield at 220℃ with 2 hours retention time, the solubilisation was mainly caused by

260 hydrolysis rather than carbonization of cellulose according to the limited change in

261 carbon content as well as HHV. In addition, the energy retention efficiency reached the

262 bottom value of 47.94% in the solid residue at 220℃ with 2 hours retention time,

263 which indicates that a large fraction of carbon was dissolved into liquid phase. This

264 finding is important as it suggested the mass change of solid residues represented the

265 solubilisation rather than carbonization extent, which on the other hand was shown by

266 the change of carbon content in the samples. Thus these two processes should be

267 carefully distinguished to determine the proper use of solid yield and carbon content

268 as two major quantitative indexes for kinetics study.

269 3.2 Kinetics study of microwave-assisted hydrothermal carbonization of cellulose

270 3.2.1 Kinetics model for MAHTC

271 $$Cellulose + H_2O \rightarrow Hydrochar + Liquid + Gas \qquad (1)$$
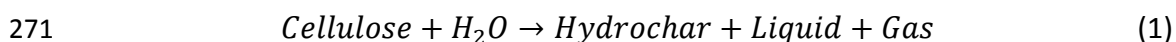
272 The HTC reaction has been described by Álvarez-Murillo et al. (2016) to match the first

273 order reaction rate mode as in Formula (1), where the volume of liquids during HTC is

274 assumed to be constant generally. In this study, the concentration of carbon was

275 introduced into calculation because when the concentration is defined in terms of

276 carbon (kg m^{-3}), it is obvious that carbon concentration of all the products come from

277 the initial carbon of cellulose, and finally results in carbon in solid (hydrochar), liquid

278 and gas phase. Since the density and dielectric constant of water drastically decreasing

279 under hydrothermal condition to form ionic liquid with gas-like density(Patel et al.,

280 2016), the products generated from feedstocks (A) in the reaction systems could be

281 divided into two categories: liquid and gas as one category (B) and hydrochar as

282 another (C). Thus the MAHTC process based on carbon concentration can be simplified

283 as Formula (2) below:

284
$$Cellulose(A) \underset{2}{\overset{1}{\diagdown}} \begin{array}{l} Liquid + Gas(B) \\ Hydrochar(C) \end{array} \qquad (2)$$
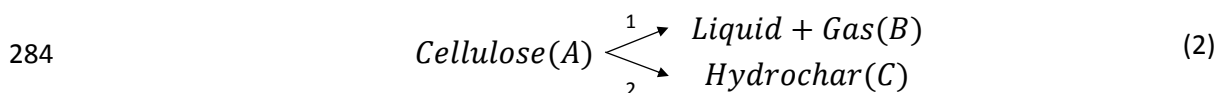
285 The first order reaction with two parallel reaction pathways in this study is in

286 accordance with the mechanism considering coexistence of 'soluble pathway' and

287 'solid pathway'. During the 'soluble pathway', it used to assume that the substrate

288   hydrolysis took place first and followed by formation of hydrochar as well as by-

289   products in the process water(Jatzwauck and Schumpe, 2015). However, the formation

290   of hydrochar from polymerization and condensation was found to take place with

291   hours of reaction time after a certain extent of hydrolysis (Hassanzadeh et al., 2014)

292   and was not observed in the experiment results of the present study. Thus the

293   formation of solid product during soluble way was negligible and therefore hydrolysis

294   process has a dominant position in the 'soluble pathway'. On the other hand, the 'solid

295   pathway' implies direct intramolecular reactions from cellulose to hydrochar, which

296   has been shown as the major mechanism route for HTC of cellulose at temperature

297   between 200-280°C (Falco et al., 2011). The two co-existent pathways are shown as

298   two different routes in Formula (2) and the kinetics is described by the following

299   different equations:

300      $\dfrac{d_{C_A}}{d_t} = -(k_1 + k_2)C_A$

301      $\dfrac{d_{C_B}}{d_t} = k_1 C_A$

302      $\dfrac{d_{C_C}}{d_t} = k_2 C_A$

303   The reactions A→B and A→C are assumed to be first order parallel reactions, where all

304   the concentration used in the equation are defined in terms of carbon (kg m^{-3}). The

305   reaction constants, k_1 and k_2, can be defined by the Arrhenius equations:

306      $k_x = k_{x,0}e^{-\frac{E_{A,x}}{RT}}$

307   Where $E_{A,x}$ is the activation energy and R is the gas constant (8.314 J mol^{-1} K^{-1}).

308   The calculation method of carbon concentration is adapted from Jatzwauck and

309   Schumpe (2015). For each hydrochar sample, the measured carbon content is defined

310   as the mean content of cellulose and hydrochar. In this way the carbon content of

311   cellulose (0.431) and hydrochar (0.725, where the highest measured carbon content is

312   defined as pure hydrochar) are used as limiting carbon content. Thus the fraction of

313   hydrochar (Y) and cellulose (1-Y) can be defined in the equation below:

314    $Carbon\ Content = 0.431(1 - Y) + 0.725Y$

315   With the result of Y, the concentration of A and C can be known based on solid

316   concentration. Thus the concentration of B can be calculated by initial carbon

317   concentration of feedstock minus C_A and C_C:

318    $Solid\ Concentration = Solid\ Yield \times \frac{m_0}{V_0} \times 10^3$ (kg m^{-3})

319    $C_A = 0.431(1 - Y) \times Solid\ Concentration$ (kg m^{-3})

320    $C_B = 0.431 \times \frac{m_0}{V_0} \times 10^3 - C_A - C_C$ (kg m^{-3})

321    $C_C = 0.725Y \times Solid\ Concentration$ (kg m^{-3})

322   Where m_0/V_0 is the initial solid concentration of 10g/300ml in the present research.

323   All the equations listed above are solved numerically by explicit Rynge-Kutta-Method

324   using ode45 function of MATLAB software.

325   3.2.2 Simulation results

326   The simulation results of evolution in carbon concentration of substrate A (Cellulose),

327   B (Liquid and gas) and C (hydrochar) under 220 to 250°C are shown in Figure 4.a-d. The

328   carbon concentration of A and C can represent the yield of each substrate respectively,

329   since the assumed carbon content of cellulose and hydrochar are of a certain value. It

330   should be noticed that from all the experimental condition, a small portion of

331   hydrochar were generated at the first stage of cellulose degradation. Thus the co-

332   existence of both 'soluble pathway' and 'solid pathway' as parallel reactions is well

333   supported. Both pathways were well described by the proposed model under all the

334   experimental conditions. The model also shows good sensitivities with respect to

335   correlation between theoretical results and experimental values.

336   Though it took relatively longer heating time to reach higher reaction temperature and

337   resulted in more solid dissolution, the HHV and carbon content showed slight change

338   under different temperature at t=0 min. Thus the starting carbon concentration of

339   substrate A showed slightly variation under different reaction temperatures because of

340   the hydrolytic breakdown of cellulose during heating process. It also explains the

341   reason that the decomposition curve of feedstock in this research was different from

342   the sigmoid curve in Álvarez's study (2016). It was inferred that decomposition rate

343   was quite slow during the heating process, then the rate begun to increase with

344   extension of reaction time reaching a maximum rate and finally the reaction

345   decelerated to reach the balance stage. Thus a sigmoid curve was formed in the cited

346   work when the heating process was taken into consideration. The simulated model

347   here was developed to describe the carbonization process that generate hydrochar,

348   which started from the middle of the sigmoid curve. It should be noted that the

349   starting concentration of substrate C, which was also the concentration of hydrochar,

350   were almost 0 kg m^{-3} at t=0 min, except the one under 250℃ was around 2 kg m^{-3}.

351 Therefore as previously explained, the impact of heating process on kinetics study of

352 carbonization process in the present model can be neglected.

353 The temperature effect on carbon conversion were shown clearly in the figures; under

354 220℃ the reaction was far from finish after 2 hours (Figure 4.a) while at 250℃ the

355 reaction reached balance within 1 hour (Figure 4.d). The increasing in curvature at

356 higher temperature were clearly observed for substrate A and C, confirming the

357 significant promoting effect of reaction temperature on reaction A→C, while the effect

358 on reaction A→B was less apparent. Thus when the reaction temperature increased

359 from 220℃ to 250℃, hydrochar had gradually become the main product instead of the

360 liquid and gas. In the same time, while the 'soluble pathway' seemed to dominate the

361 process at 220℃, the 'solid pathway' became the predominant mechanism when

362 temperature exceeded 230℃. Results from elemental analysis was in good agreement

363 with the simulation model that reaction temperature played a great role in

364 determining the predominant kinetics(Lu et al., 2013). Though the dehydration process

365 was observed under all reaction temperatures, the differences in the reaction extents

366 could not be ignored. The explanation can be that under both 'soluble pathway' and

367 'solid pathway', cellulose would undergo dehydration process from intermolecular and

368 intramolecular respectively, resulting in the liquid intermediate products as well as the

369 aromatic hydrochar samples (Falco et al., 2011). The change trend of atomic ratios also

370 suggested dehydration took place during HTC with decarboxylation and deoxygenating

371 coexisting simultaneously, which is similar with published results of traditional HTC(Lu

372 et al., 2013).

373   3.2.3 Analysis of parameters

374   The simulating values of two first-order rate constants are listed in Table 1. An

375   Arrhenius plot from both k_1 and k_2 is shown in Figure 5 to obtain the optimized

376   parameters values, which are listed in Table 3 as well. The calculated activation

377   energies are 53.0 kJ mol^{-1} and 198.1 kJ mol^{-1}, for 'soluble pathway' and 'solid pathway'

378   respectively. The category $k_1 + k_2$ describes the decomposition of cellulose as a

379   pseudo-first order reaction with activation energy of 147.8 kJ mol^{-1}. All three linear fit

380   show good consistence with R^2 over 0.97. Comparison of k_1 and k_2 shows the

381   predominant pathway under different temperature, i.e. at 220℃ k_1 is higher than k_2,

382   indicating the degradation of cellulose mainly went through hydrolysis reaction. On the

383   contrary, k_2 increased faster and surpassed k_1 when the 'solid pathway' was majorly

384   involved under high reaction temperature. These results are in great agreement with

385   the process analytical results based on characteristics of hydrochar, which is evident to

386   prove that HTC undergoes hydrolysis and carbonization process as two parallel

387   reactions as a result of the acceleration effects from microwave heating. The results

388   also agree with García-Bordejé et.al (2017) that the predominant mechanism depends

389   on variations in the individual rates of these two co-existent pathways, which is the

390   'soluble pathway' at 220℃ and 'solid pathway' at its favourable high temperatures

391   (230-250℃).

392   The previous reported activation energy value of 'soluble pathway' was 90.1 kJ mol^{-1}

393   (Álvarez-Murillo et al., 2016) and 77 kJ mol^{-1} (Reza et al., 2013), where the hydrochar

394   were defined as a first order degradation product of cellulose as well as liquid and gas

18

395   products. There was no reported activation energy value of a separate hydrolysis

396   process in HTC except the lumped model for HTC of soft rash by Jatzwauck and

397   Schumpe (2015) with a much higher value of 141 kJ mol^{-1}. The calculated activation

398   energy in this study is much lower (53.0 kJ mol^{-1}), which can be explained by the

399   ignorance of hydrochar formation under 'soluble pathway' as well as the promoted

400   hydrolysis efficiency with the assistance of microwave(Fan et al., 2013). As for the

401   'solid pathway', the resulting activation energy was 198.1 kJ, much higher than the

402   'soluble pathway'. Thus the 'solid pathway' was proved to favour high reaction

403   temperature, which made it the predominant mechanism for carbonization under 230-

404   250℃. This high value is well supported by the energy consuming pyrolysis-like

405   intramolecular reactions under 'solid pathway' as previous explained. The calculated

406   aviation energy was a bit lower than that of cellulose pyrolysis in absence of water,

407   which was about 227 to 242 kJ mol^{-1} (Lédé, 2012). It was mainly due to the less stable

408   structure of hydrochar samples obtained during MAHTC than chars generated from

409   pyrolysis. The explanation of how the cellulose undergoes similar reactions during HTC

410   in a lower temperature range than pyrolysis is possibly because of the autogenous high

411   pressure (25-30 bar) (Falco et al., 2011).

412   The decomposition of cellulose is defined as a pseudo-first order reaction in this study

413   with relatively lower activation energy of 147.8 kJ mol^{-1}. Peterson et al. (2008)

414   summarized previous data of cellulose degradation in hydrothermal media as first

415   order reaction and resulted in a best-fit line with an activation energy of 215 kJ mol^{-1}.

416   With a clear decrease in activation energy, the results from this study agreed with

417   those reported previously that the activation energy to provoke the cellulose

418 degradation was easier to achieve with high microwave densities(Fan et al., 2013). A

419 possible explanation is the higher energy efficiency provided during microwave heating

420 than conventional heating, which in the meantime resulted in energy-favourable

421 hydrochar within evident shortened reaction time.

422 The role that microwave played during MAHTC could be explained by its activation of

423 CH_2OH groups and crystalline content of cellulose above 220℃ according to the

424 interaction mechanism proposed by Fan et al. (2013). It was also reported that high

425 liquefaction yield could be achieved under mild hydrothermal conditions(Hassanzadeh

426 et al., 2014) when the CH_2OH groups act as 'molecular radiators' in the presence of

427 microwave(Fan et al., 2013). In this study, not only hydrolysis process, but also

428 carbonization process was proved to be promoted. The promotion effect of microwave

429 was explained by observed higher heating rates during pre-experiments because

430 microwave energy is transformed into thermal energy inside the particle(Patel et al.,

431 2016). By contract only surface heating transformation occurs under conventional

432 hydrothermal conditions. The inner-particle energy transformation provided by

433 microwave heating further accelerated the carbonization process and made the

434 transformation more close to pyrolysis, resulting in the predominant 'solid pathway'

435 under MAHTC. The previously reported higher thermochemical decomposition of

436 various biomass feedstocks(Zhang et al., 2017) during microwave assisted pyrolysis

437 than conventional pyrolysis can be supportive for this result. It can be assumed that

438 the intramolecular reactions are enhanced since microwave could interact with the

439 feedstock particles, therefore resulting in hydrochar generation after fast dehydration

440 process.

When it comes to the real biomass samples, the thermal behaviour can be more complicated due to the presence of other components like lignin and hemicellulose. It has been discussed in previous researches(Elaigwu, 2016; Kim et al., 2016) that these three main components of biomass waste have different thermal stability. Microwave was shown to have more significant effects on reducing the cellulose band rather than lignin aromatic systems according to the FTIR results of biochars generated from microwave and slow pyrolysis (Mašek et al., 2013). Thus it is reasonable to hypothesize that the real biomass samples would be less degraded comparing to cellulose under the proposed reaction condition in this study, leading to higher solid yield as a consequence. In the meantime, the amount of volatiles compounds can also contribute to the solid yields due to some side reactions after released from degradation process(Guiotoku et al., 2009). However, the existing results of comparison between microwave assisted conventional HTC of biomass and other biowaste have already shown the promising side of MAHTC, which are the improved processing rate and lower energy requirement to reach similar extent of transformation. Further research can be conducted between different biomass samples with various composition to give advises on practical application of MAHTC.

4. Conclusion

Microwave heating was demonstrated to be a useful method to assist hydrothermal carbonization treatment. The optimized condition for energy-enriched products in this research was 250℃ for 90 min, considering both hydrochar properties and energy retention efficiency. Kinetics study and experimental analysis were in agreement that

463 illustrated the predominant mechanism of the reaction depend on variations in the

464 reaction rates of two co-existent pathways. Results from the calculated activation

465 energies further proved the pyrolysis-like intramolecular reactions under 'solid

466 pathway' dominated the mechanism under high temperatures and showed the

467 positive effects of microwave heating on hydrothermal degradation of cellulose.

468 (E-supplementary data for this work includes figures that illustrate the characteristics

469 of the microwave-assisted hydrothermal carbonization reactor, correlation assessment

470 of the presented model and calculated atomic H/C and O/C ratios, which can be found

471 in e-version of this paper online.)

476 **References**

477 1. Afolabi, O.O.D., Sohail, M., Thomas, C.L.P. 2017. Characterization of solid fuel chars

478 recovered from microwave hydrothermal carbonization of human biowaste. *Energy*,

479 **134**, 74-89.

480 2. Álvarez-Murillo, A., Sabio, E., Ledesma, B., Román, S., González-García, C.M. 2016.

481 Generation of biofuel from hydrothermal carbonization of cellulose. Kinetics

482 modelling. *Energy*, **94**(Supplement C), 600-608.

483   3. Berge, N.D., Li, L., Flora, J.R.V., Ro, K.S. 2015. Assessing the environmental impact of

484   energy production from hydrochar generated via hydrothermal carbonization of food

485   wastes. *Waste Management*, **43**, 203-217.

486   4. Berge, N.D., Ro, K.S., Mao, J., Flora, J.R., Chappell, M.A., Bae, S. 2011. Hydrothermal

487   carbonization of municipal waste streams. *Environ Sci Technol*, **45**(13), 5696-703.

488   5. Danso-Boateng, E., Holdich, R.G., Shama, G., Wheatley, A.D., Sohail, M., Martin, S.J.

489   2013. Kinetics of faecal biomass hydrothermal carbonisation for hydrochar production.

490   *Applied Energy*, **111**(Supplement C), 351-357.

491   6. de la Hoz, A., Diaz-Ortiz, A., Moreno, A. 2005. Microwaves in organic synthesis.

492   Thermal and non-thermal microwave effects. *Chemical Society Reviews*, **34**(2), 164-

493   178.

494   7. Diakité, M., Paul, A., Jäger, C., Pielert, J., Mumme, J. 2013. Chemical and

495   morphological changes in hydrochars derived from microcrystalline cellulose and

496   investigated by chromatographic, spectroscopic and adsorption techniques.

497   *Bioresource Technology*, **150**(Supplement C), 98-105.

498   8. Elaigwu, S.E., Greenway, G.M. 2016. Microwave-assisted and conventional

499   hydrothermal carbonization of lignocellulosic waste material: Comparison of the

500   chemical and structural properties of the hydrochars. *Journal of Analytical & Applied*

501   *Pyrolysis*, **118**, 1-8.

502   9. Elaigwu, S.E.G., Gillian M. 2016. Microwave-assisted hydrothermal carbonization of

503   rapeseed husk: A strategy for improving its solid fuel properties. *Fuel Processing*

504   *Technology*, **149**, 305-312.

505   10. Falco, C., Baccile, N., Titirici, M.M. 2011. Morphological and structural differences

506   between glucose, cellulose and lignocellulosic biomass derived hydrothermal carbons.

507   *Green Chemistry*, **13**(11), 3273-3281.

508   11. Fan, J., Bruyn, M.D., Budarin, V.L., Gronnow, M.J., Shuttleworth, P.S., Breeden, S.,

509   Macquarrie, D.J., Clark, J.H. 2013. Direct Microwave-Assisted Hydrothermal

510   Depolymerization of Cellulose. *Journal of the American Chemical Society*, **135**(32),

511   11728.

512   12. Fava, F., Totaro, G., Diels, L., Reis, M., Duarte, J., Carioca, O.B., Poggi-Varaldo, H.M.,

513   Ferreira, B.S. 2015. Biowaste biorefinery in Europe: opportunities and research &

514   development needs. *New Biotechnology*, **32**(1), 100-108.

515   13. García-Bordejé, E., Pires, E., Fraile, J.M. 2017. Parametric study of the

516   hydrothermal carbonization of cellulose and effect of acidic conditions. *Carbon*,

517   **123**(Supplement C), 421-432.

518   14. Goto, M., Obuchi, R., Hirose, T., Sakaki, T., Shibata, M. 2004. Hydrothermal

519   conversion of municipal organic waste into resources. *Bioresource Technology*, **93**(3),

520   279-284.

521   15. Guiotoku, M., Rambo, C.R., Hansel, F.A., Magalhães, W.L.E., Hotza, D. 2009.

522   Microwave-assisted hydrothermal carbonization of lignocellulosic materials. Materials

523   Letters, 63(30), 2707-2709.

524   16. Hassanzadeh, S., Aminlashgari, N., Hakkarainen, M. 2014. Chemo-selective high

525   yield microwave assisted reaction turns cellulose to green chemicals. *Carbohydrate*

526   *Polymers*, **112**(Supplement C), 448-457.

527 17. Hassanzadeh, S., Aminlashgari, N., Hakkarainen, M. 2015. Microwave-Assisted

528 Recycling of Waste Paper to Green Platform Chemicals and Carbon Nanospheres. *Acs*

529 *Sustainable Chemistry & Engineering*, **3**(1), 177-185.

530 18. Hoekman, S.K., Broch, A., Robbins, C. 2011. Hydrothermal Carbonization (HTC) of

531 Lignocellulosic Biomass. *Energy Fuels*, **25**(4), 1802-1810.

532 19. Jatzwauck, M., Schumpe, A. 2015. Kinetics of hydrothermal carbonization (HTC) of

533 soft rush. *Biomass and Bioenergy*, **75**(Supplement C), 94-100.

534 20. Kambo, H.S., Dutta, A. 2014. Strength, storage, and combustion characteristics of

535 densified lignocellulosic biomass produced via torrefaction and hydrothermal

536 carbonization. *Applied Energy*, **135**, 182-191.

537 21. Kang, S., Li, X., Fan, J., Chang, J. 2012. Characterization of Hydrochars Produced by

538 Hydrothermal Carbonization of Lignin, Cellulose, d-Xylose, and Wood Meal. *Industrial*

539 *& Engineering Chemistry Research*, **51**(26), 9023–9031.

540 22. Kannan, S., Gariepy, Y., Raghavan, G.S.V. 2017. Optimization and characterization

541 of hydrochar produced from microwave hydrothermal carbonization of fish waste.

542 *Waste Management*, **65**(Supplement C), 159-168.

543 23. Kim, D., Lee, K., Park, K.Y. 2016. Upgrading the characteristics of biochar from

544 cellulose, lignin, and xylan for solid biofuel production from biomass by hydrothermal

545 carbonization. *Journal of Industrial & Engineering Chemistry*, **42**, 95-100.

546 24. Klein, M., Griess, O., Pulidindi, I.N., Perkas, N., Gedanken, A. 2016. Bioethanol

547 production from Ficus religiosa leaves using microwave irradiation. *Journal of*

548 *Environmental Management*, **177**, 20.

549   25. Lédé, J. 2012. Cellulose pyrolysis kinetics: An historical review on the existence and

550   role of intermediate active cellulose. *Journal of Analytical and Applied Pyrolysis*,

551   **94**(Supplement C), 17-32.

552   26. Lu, X., Jordan, B., Berge, N.D. 2012. Thermal conversion of municipal solid waste

553   via hydrothermal carbonization: Comparison of carbonization products to products

554   from current waste management techniques. *Waste Management*, **32**(7), 1353-1365.

555   27. Lu, X., Pellechia, P.J., Flora, J.R., Berge, N.D. 2013. Influence of reaction time and

556   temperature on product formation and characteristics associated with the

557   hydrothermal carbonization of cellulose. *Bioresour Technol*, **138**, 180-90.

558   28. Lynam, J.G., Reza, M.T., Yan, W., Vásquez, V.R., Coronella, C.J. 2014. Hydrothermal

559   carbonization of various lignocellulosic biomass. *Biomass Conversion and Biorefinery*,

560   **5**(2), 173-181.

561   29. Mašek, O., Budarin, V., Gronnow, M., Crombie, K., Brownsort, P., Fitzpatrick, E.,

562   Hurst, P. 2013. Microwave and slow pyrolysis biochar—Comparison of physical and

563   functional properties. Journal of Analytical and Applied Pyrolysis, 100, 41-48.

564   30. Ood, A., Sohail, M. 2017. Comparative evaluation of conventional and microwave

565   hydrothermal carbonization of human biowaste for value recovery. *Water Science &*

566   *Technology*, wst2017164.

567   31. Patel, B., Guo, M., Izadpanah, A., Shah, N., Hellgardt, K. 2016. A review on

568   hydrothermal pre-treatment technologies and environmental profiles of algal biomass

569   processing. *Bioresource Technology*, **199**(Supplement C), 288-299.

570   32. Peterson, A.A., Vogel, F., Lachance, R.P., Froling, M., Antal, J.M.J., Tester, J.W.

571   2008. Thermochemical biofuel production in hydrothermal media: A review of sub-

572   and supercritical water technologies. *Energy & Environmental Science*, **1**(1), 32-65.

573   33. Reza, M.T., Yan, W., Uddin, M.H., Lynam, J.G., Hoekman, S.K., Coronella, C.J.,

574   Vasquez, V.R. 2013. Reaction kinetics of hydrothermal carbonization of loblolly pine.

575   *Bioresour Technol*, **139**, 161-9.

576   34. Richel, A., Laurent, P., Wathelet, B. 2011. Microwave-assisted conversion of

577   carbohydrates. State of the art and outlook. *Comptes Rendus Chimie*, **14**(2-3), 224-234.

578   35. Sevilla, M., Fuertes, A.B. 2009. The production of carbon materials by

579   hydrothermal carbonization of cellulose. *Carbon*, **47**(9), 2281-2289.

580   36. Suhas, Gupta, V.K., Carrott, P.J.M., Singh, R., Chaudhary, M., Kushwaha, S. 2016.

581   Cellulose: A review as natural, modified and activated carbon adsorbent. *Bioresource*

582   *Technology*, **216**(Supplement C), 1066-1076.

583   37. Zhang, Y., Chen, P., Liu, S., Peng, P., Min, M., Cheng, Y., Anderson, E., Zhou, N., Fan,

584   L., Liu, C., Chen, G., Liu, Y., Lei, H., Li, B., Ruan, R. 2017. Effects of feedstock

585   characteristics on microwave-assisted pyrolysis – A review. *Bioresource Technology*,

586   **230**(Supplement C), 143-151.

587